ELSEVIER

Polymer 42 (2001) 6871–6876

polymer

www.elsevier.nl/locate/polymer

Controllable interaction between cations and thermally sensitive poly(*N*-vinylcaprolactam-*co*-sodium acrylate) microgels in water

Shufu Peng[a], Chi Wu[b,*]

[a]*The Open Laboratory of Bond-selective Chemistry, Department of Chemical Physics, University of Science and Technology of China, Hefei, Anhui, People's Republic of China*

[b]*Department of Chemistry, The Chinese University of Hong Kong, Shatin, Hong Kong*

Received 27 November 2000; received in revised form 14 February 2001; accepted 16 February 2001

Abstract

The microgels made of poly(*N*-vinylcaprolactam) (PVCL) and a few percent of sodium acrylate (SA) were used as a model system to study the cation induced aggregation of colloid particles. Using such microgels make the aggregation controllable and reversible because PVCL can gradually change from hydrophilic (soluble) to hydrophobic (insoluble) in water when the temperature is increased in the range 25–35°C. The aggregation induced by different kinds of cations and at different temperatures was investigated by using a combination of static and dynamic laser light scattering (LLS). At temperatures lower than ~30°C, the microgel shrinks with increasing the cation concentration due to the increase in the ionic strength and the intra-microgel complexation. The extent of the shrinking induced by different cations follows the order of $Hg^{2+} \gg Cu^{2+} > Ca^{2+} > Na^{+}$. At temperatures higher than ~32°C, Ca^{2+} and Cu^{2+} can induce inter-microgel aggregation. The Ca^{2+} induced aggregation is essentially reversible in the heating-and-cooling cycle, but there exists a large hysteresis in the Cu^{2+} induced one. As expected, monovalent Na^{+} was not able to induce the inter-microgel aggregation. The complexation between Hg^{2+} and carboxylic groups is so strong that the intra-microgel complexation becomes so dominant that Hg^{2+} was also not able to induce the inter-microgel aggregation.

Keywords: Microgel; Controllable association; Thermally sensitive gels

1. Introduction

The study of cation/polyanion association/interaction is important in understanding various physicochemical behaviors in environmental research and biological science. Such an association also has many direct technological applications. Experimental observation is usually related to an overall distribution of cations around polyanion chains without knowing how various fractions are attributed to different underlying interaction processes, such as electrostatic repulsion and complexation [1]. It is known that certain alkaline earth ions and heavy metal ions can specifically interact with carboxylic groups [2,3]. If carboxylic groups are attached to a polymer chain backbone, as in polyacrylic acid and its copolymers, this interaction can lead to the cation/polyanion 'complexation' even at a very low cation concentration [4,5]. Furthermore, some polyanions can complex with protein, in which metal ions are acted as cross-linking agents. Long time ago, Wall and Drenan [6] investigated the Ca^{2+}, Ba^{2+} and Sr^{2+} induced precipitation of polyacrylates and interpreted their results as gelation via the bond formation between the polyelectrolyte chains and cations. Flory et al. [7] pointed out that Ca^{2+} could induce a much profound chain contraction of partly neutralized polyacrylates than an equivalent amount of Na^{+}. Recent studies have revealed some important roles of metal ions, such as Cu^{2+}, Zn^{2+} and Fe^{3+}, in the functional activity of immunocomponent cells [8–11]. It has been suggested that the addition of metal ions to an aqueous solution of polyanions could alternate the hydration, i.e. disrupting oriented water molecules near the polymer chain [12–14]. Our recent study showed that there existed a competition between the intrachain and interchain Ca^{2+}/polyanion interactions [15]. The transition from the domination of one interaction to another can be used to alternate the structure of the aggregates.

In this study, narrowly distributed spherical microgels made of lightly cross-linked poly(*N*-vinylcaprolactam) (PVCL) chains copolymerized with a few percent of sodium acrylate [P(VCL-*co*-SA)] were prepared by precipitation polymerization. Using P(VCL-*co*-SA) microgels has the

* Corresponding author. Tel.: +852-2609-6106; fax: +852-2603-5057.
E-mail address: chiwu@cuhk.edu.hk (C. Wu).

0032-3861/01/$ - see front matter
PII: S0032-3861(01)00174-4

Table 1
LLS results of P(VCL-*co*-SA) microgels in different 0.01N cation solutions at 25°C. Relative errors: $\langle R_h \rangle$, ±2%; $\langle R_g \rangle$, ±5%; $\langle R_g \rangle / \langle R_h \rangle$, ±7%; $M_{w,microgel}$, ±5%

Cationic ions	$\langle R_h \rangle$ (nm)	$\langle R_g \rangle$ (nm)	$\langle R_g \rangle / \langle R_h \rangle$	$M_{w,microgel}/10^{-}8$ (g/mol)
No cation	258	221	0.86	8.3
Na^+	242	216	0.89	8.5
Ca^{2+}	237	200	0.85	8.9
Cu^{2+}	223	180	0.81	8.4
Hg^{2+}	195	146	0.75	8.0

following advantages: (1) thermally sensitive PVCL in water can gradually and reversibly change from hydrophilic (soluble) to hydrophobic (insoluble) when the temperature is increased in the range 25–35°C [16–18], which enables us to use a simple temperature variation to induce and control the aggregation of the microgels via a combination of hydrophobic interaction and the cation/polyanions complexation; and (2) spherical microgels have a better defined shape in comparison with linear chains. Moreover, the cation induced microgel aggregation can be used to prepare a novel hybrid gel composition. The present study is a fundamental study of some envisioned biomedical applications, such as the immobilization of proteins and drugs.

2. Experimental

2.1. Materials

N-vinylcaprolactam monomer (VCL, courtesy of BASF) was purified by reduced pressure distillation. Sodium acrylate monomer (SA, from Lancaster) was used without further purification. Potassium persulfate as an initiator (KPS, from Aldrich) and *N*,*N*′-methylenebisacrylamide as a cross-linking agent (MBAA, from Aldrich) were recrystallized three times in methanol. Sodium chloride (NaCl, from BDH), calcium chloride (Anhydrous $CaCl_2$, from ACROS), copper chloride ($CuCl_2$, from Aldrich), and mercury chloride ($HgCl_2$, from BDH) were used without further purification.

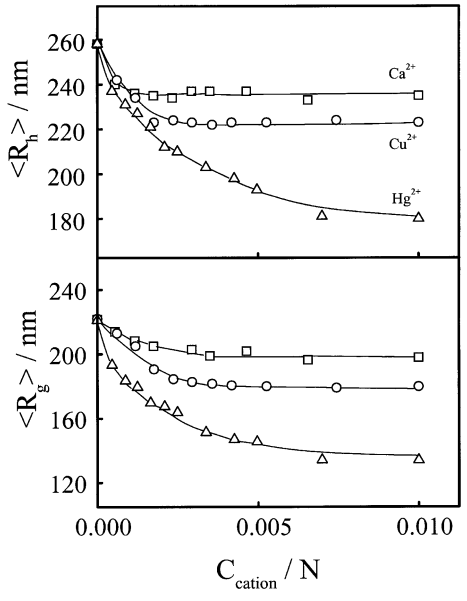

Fig. 1. The cation molar concentration dependence of average hydrodynamic radius $\langle R_h \rangle$ and average radius of gyration $\langle R_g \rangle$ of P(VCL-*co*-SA) microgels at 25°C.

2.2. Sample preparation

Spherical poly(*N*-vinylcaprolactam-*co*-sodium acrylate) microgels were prepared by precipitation polymerization. Into a 150 ml three-neck flask equipped with a reflux condenser, a thermometer and a nitrogen-bubbling tube, were added VCL monomer (7.3 mmol), SA comonomer (0.37 mmol), MBAA cross-linking (0.18 mmol) and deionized water (40 ml). The solution was stirred and bubbled by nitrogen for 1 h to remove oxygen before adding an aqueous solution of KPS (0.05 mmol) to initiate the polymerization at 60°C for 24 h. The resultant P(VCL-*co*-SA) microgel was purified by a successive four cycles of centrifugation (Sigma 2K15 ultracentrifuge, at 15,300 rpm and 40°C), decantation and redispersion in deionized water to remove unreacted low molar mass molecules. The microgels on average contained 4.3 mol% acrylic groups.

2.3. Laser light scattering (LLS)

The detail of our LLS spectrometer can be found elsewhere [19]. In static LLS, the angular dependence of the absolute excess time-averaged scattered intensity, known as the Rayleigh ratio $R_{vv}(q)$, is related to the weight-average molar mass (M_w), the *z*-average root-mean-square radius of gyration ($\langle R_g^2 \rangle_z^{1/2}$ or written as $\langle R_g \rangle$) and the second virial coefficient (A_2) of the scattering objects

$$\frac{KC}{R_{vv}(q)} \cong \frac{1}{M_w}\left(1 + \frac{1}{3}\langle R_g^2 \rangle_z q^2\right) + 2A_2C, \quad (1)$$

where $q = (4\pi n/\lambda)\sin(\theta/2)$ with n, λ and θ being the refractive index of solvent, the wavelength of the light in vacuum and the scattering angle, respectively. In dynamic LLS, the cumulant or Laplace inversion analysis of the measured intensity–intensity time correlation function $G^{(2)}(q,t)$ in the self-beating mode can lead to an average line width ($\langle \Gamma \rangle$) or a line width distribution ($G(\Gamma)$) [20,21]. For a pure diffusive relaxation, Γ can be related to the translational diffusion coefficient D via $\Gamma = Dq^2$ at $C \rightarrow 0$ and $q \rightarrow 0$ [22], or the hydrodynamic radius (R_h) by the Stokes–Einstein equation, $D = k_B T/(6\pi\eta R_h)$, where k_B, T and η are the Boltzmann constant, the absolute temperature and the solvent viscosity, respectively.

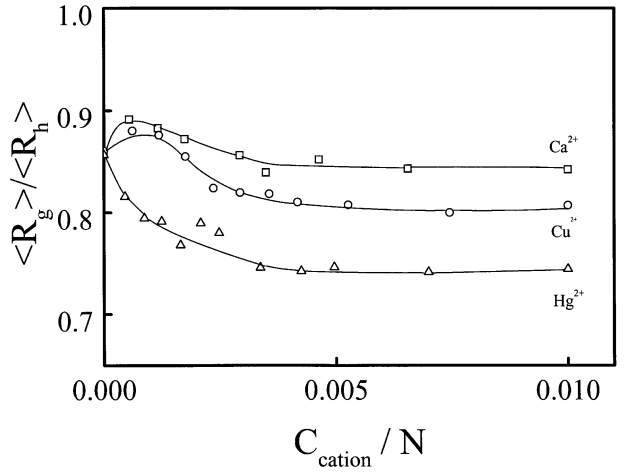

Fig. 2. The cation molar concentration dependence of ratio of average radius of gyration to average hydrodynamic radius $\langle R_g\rangle/\langle R_h\rangle$ of P(VCL-*co*-SA) microgels at 25°C.

3. Results and discussion

Table 1 summarizes the LLS results of P(VCL-*co*-SA) microgels in deionized water and in different 0.01N salt solutions. It is clear that Na^+ has the weakest effect on the microgels, while Hg^{2+} leads to a profound shrinking. This is understandable because the presence of monovalent Na^+ can only increase the ionic strength and reduce electrostatic repulsion between carboxylic groups. Besides the influence on the ionic strength, divalent cations can also pull two carboxylic groups together so that they can induce a larger shrinking of the microgels. The fact that the molar mass of the microgels ($M_{w,microgel}$) remains a constant indicates no interparticle complexation, or in other words, the interaction between cations and microgels at 25°C is purely intra-microgel. The decrease of $\langle R_g\rangle/\langle R_h\rangle$ indicates that the shrinking of the microgel reduces the hydrodynamic draining.

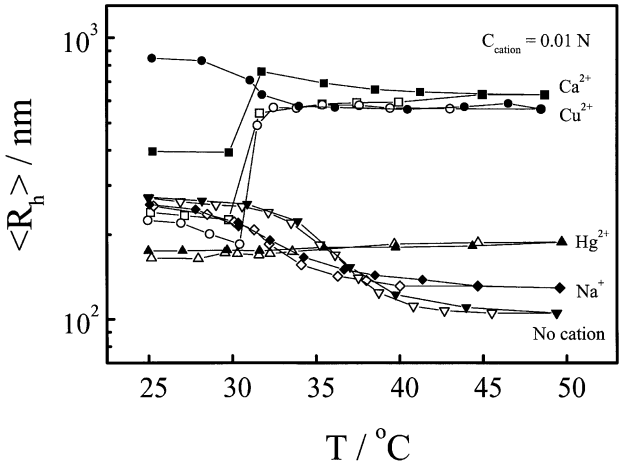

Fig. 3. Temperature dependence of average hydrodynamic radius $\langle R_h\rangle$ of P(VCL-*co*-SA) microgels, where cation concentration is 0.01N, where the open symbols represent the heating process, while the filled symbols are for the cooling process.

Table 1 shows that in terms of the effect of different cations on the shrinking of the microgels, $Hg^{2+} \gg Cu^{2+} > Ca^{2+}$. Such an effect can be better viewed in terms of the cation concentration dependence of $\langle R_g\rangle$ and $\langle R_h\rangle$.

Fig. 1 shows a clear shrinking of the microgels as the cation concentration is increased. There exist at least four interactions in the mixture of cations and polyanions: the hydrophobic attraction among the hydrocarbon backbone chains, the hydration of the polymer chain, the electrostatic repulsion between carboxylic groups, and the electrostatic attraction (or complexation) among divalent cations and carboxylic groups. The balance of these interactions determines whether the microgel is in the swelling or shrinking state. It is clear that the addition of cations not only increases the ionic strength (reduces the electrostatic repulsion), but also leads to possible complexation, depending on the kind of cation used. The shrinking of the microgels can also be viewed in terms of the ratio of $\langle R_g\rangle/\langle R_h\rangle$. It is known that for a uniform non-draining sphere, $\langle R_g\rangle/\langle R_h\rangle \sim 0.774$. The hydrodynamic draining results in a relatively smaller $\langle R_h\rangle$ and a large ratio of $\langle R_g\rangle/\langle R_h\rangle$.

Fig. 2 shows that $\langle R_g\rangle/\langle R_h\rangle$ decreases as the cation concentration is increased, indicating that the shrinking of the microgels reduces the hydrodynamic draining. When the cation concentration reaches ~0.005N, $\langle R_g\rangle/\langle R_h\rangle$ approaches different constants in the presence of different cations. Note that for Ca^{2+} and Cu^{2+}, $\langle R_g\rangle/\langle R_h\rangle$ increases slightly in the low cation concentration range. A comparison between the decreases of $\langle R_g\rangle$ and $\langle R_h\rangle$ in Fig. 1 shows that $\langle R_h\rangle$ decreases faster than $\langle R_g\rangle$ in this range. This could be attributed to the collapse of the rough surface of the microgel. Fig. 2 shows that Hg^{2+} is most effective in inducing the shrinking and reducing the hydrodynamic draining. As $[Hg^{2+}]$ is increased, $\langle R_g\rangle/\langle R_h\rangle$ decreases from 0.86 to ~0.75, indicating that the microgels are collapsed and becomes non-draining at $[Hg^{2+}] >$ ~0.0025N.

Figs. 3 and 4 show the temperature dependence of the average hydrodynamic radius $\langle R_h\rangle$ and the weight average molar mass $M_{w,aggregate}$ of the P(VCL-*co*-SA) microgels, respectively, in the heating and cooling. Note that in the presence of Na^+, $\langle R_h\rangle$ gradually decreases as the temperature is increased, but the molar mass remains to be a constant, indicating that there is no inter-microgel aggregation. The shrinking of individual microgels is due to the intra-microgel hydrophobic attraction. The addition of Ca^{2+} or Cu^{2+} leads to different results; namely, in the range 25–32°C, the shrinking of microgels is similar to the case of adding Na^+, but when the temperature reaches ~32°C, the sharp increases of $\langle R_h\rangle$ and $M_{w,aggregate}$ clearly reveal an inter-microgel aggregation. However, in the presence of Hg^{2+}, both $\langle R_h\rangle$ and $M_{w,aggregate}$ are nearly independent of temperature. Presumably, the inter-microgel aggregation is induced by the attraction between one cation and two anionic carboxylic groups on two different microgels. In the presence of 0.01N Ca^{2+} or Cu^{2+}, each aggregate on average, contains ~100–200 microgels. The different

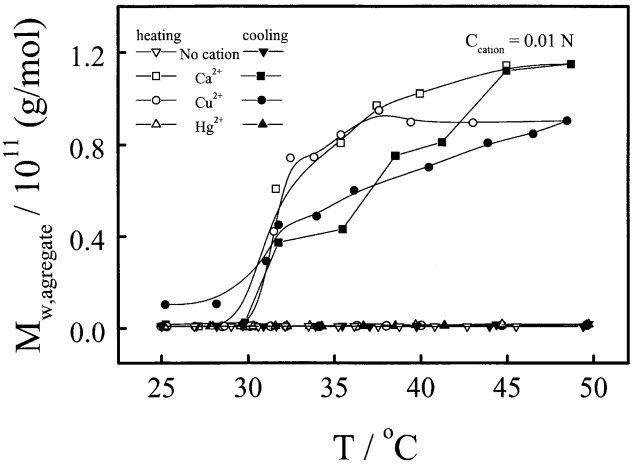

Fig. 4. Temperature dependence of weight average molar mass $M_{w,aggregate}$ of P(VCL-*co*-SA) microgels, where cation concentration is 0.01N.

effects of Na^+, Ca^{2+}, Cu^{2+} and Hg^{2+} on the microgels can be explained as follows.

When the temperature reaches the transition temperature, the PVCL chains become hydrophobic and start to collapse, but the hydrophilic COO^- groups tend to stay on the periphery. In the case of Na^+, there is no complexation between COO^- and Na^+, so that Na^+ is not able to pull different microgels together, while in the case of Ca^{2+} and Cu^{2+}, the attraction/complexation among one cation and two COO^- groups on the surface of two different microgels leads to the aggregation. As for the case of Hg^{2+}, the strong intra-microgel complexation results in a complete intra-microgel complexation so that the microgel collapses even at 25°C. Therefore, no sufficient amount of carboxylic groups are left on its periphery to induce the inter-microgel complexation.

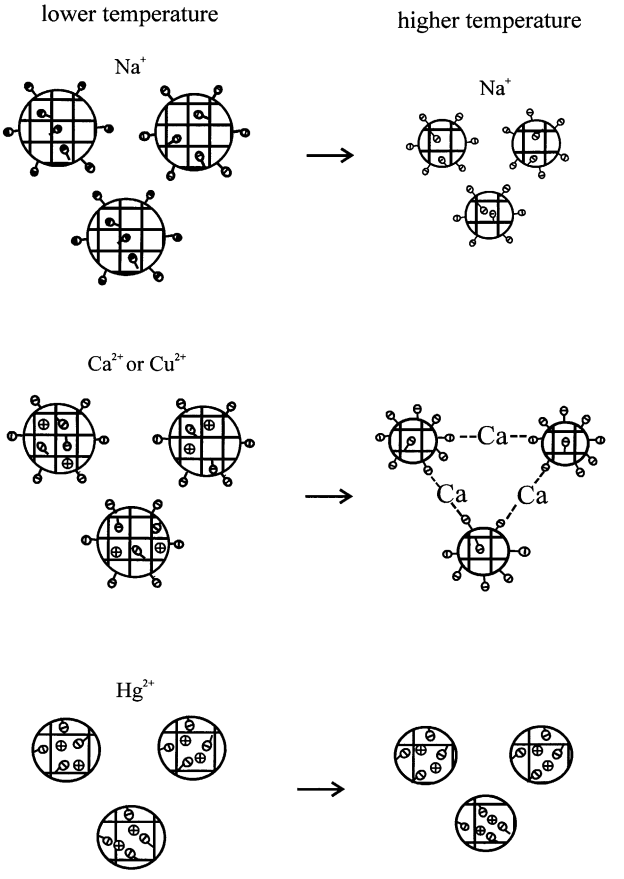

Fig. 5. Schematic of effects of different cations and temperature on the P(VCL-*co*-SA) microgels.

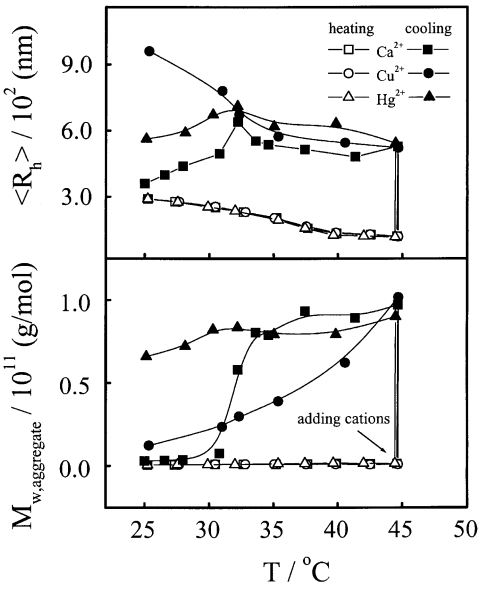

Fig. 6. Temperature dependence of average hydrodynamic radius $\langle R_h \rangle$ and weight average molar mass $M_{w,aggregate}$ of P(VCL-*co*-SA) microgels, where cations were added after the temperature was risen to 45°C.

Figs. 3 and 4 also show the cation and temperature dependence of $\langle R_h \rangle$ and $M_{w,aggregate}$ of the aggregates in the cooling processes. A comparison of the heating and cooling processes shows that there exists a hysteresis in the first heating and cooling cycle. It is interesting to note that before dropping at ~32°C, $\langle R_h \rangle$ slightly increases in the cooling, revealing the swelling of individual microgel inside the aggregate. When $T < \sim 32$°C, individual swollen microgels become so hydrophilic that the strength of the attraction between Ca^{2+} and the COO^- groups on the periphery is not sufficient to pull different microgels together, so that most of the aggregates are dissociated at 25°C. In the case of Cu^{2+}, $\langle R_h \rangle$ increases in the cooling even at temperature lower than 32°C, revealing that the attraction between Cu^{2+} and COO^- groups is so strong that the dissociation of the aggregates is incomplete. The hystersis in the change of $M_{w,aggregate}$ in Fig. 4 also shows that the dissociation of the aggregate at lower temperatures is not complete. As expected, for the case of Na^+ and Hg^{2+}, there is no hystersis in the cooling. However, as we discussed before, the reasons for the temperature independence in these two cases are completely different. Fig. 5 shows a schematic diagram of the effects of different cations and temperature on the P(VCL-*co*-SA) microgels.

In order to prove that it is those COO^- groups on the

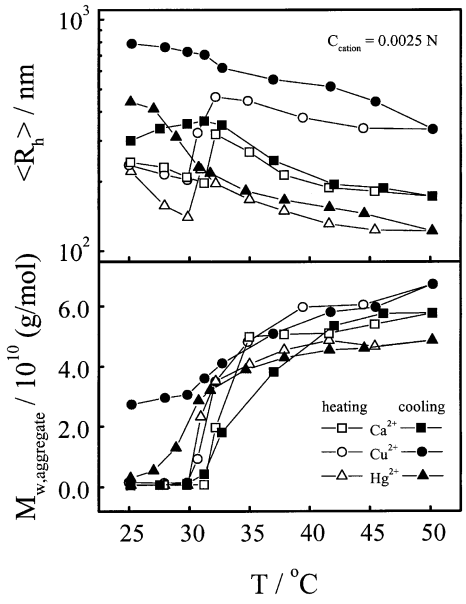

Fig. 7. Temperature dependence of average hydrodynamic radius $\langle R_h \rangle$ and weight average molar mass $M_{w,aggregate}$ of P(VCL-*co*-SA) microgels, where cation concentration is 0.0025N.

periphery that lead to the inter-microgel aggregation. We changed the order of adding cations and rising the temperature; namely, we first increased the temperature higher than 32°C and then added different cations. Fig. 6 shows that after 0.01N cations were added at 45°C, both $\langle R_h \rangle$ and $M_{w,aggregate}$ increased sharply, clearly showing that adding cations before or after increasing the temperature had completely different results. It supports our argument that at higher temperatures, the collapse of the microgel forces the COO^- groups to stay on

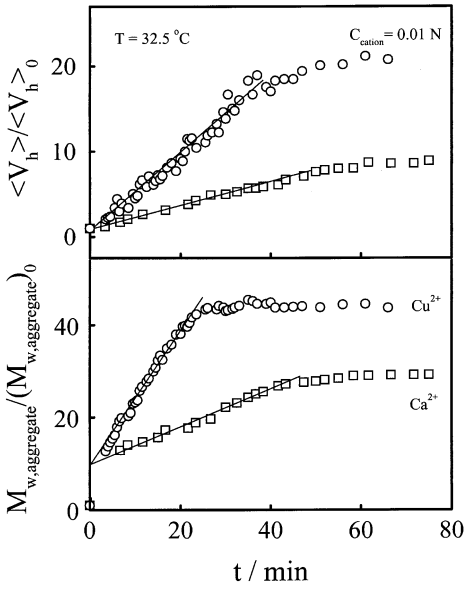

Fig. 8. Time dependence of relative average hydrodynamic volume $\langle V_h \rangle / \langle V_h \rangle_0$ and relative weight average molar mass $M_{w,aggregate}/(M_{w,aggregate})_0$ of P(VCL-*co*-SA) microgels after the temperature of the dispersion was increased from 25 to 32.5°C, where cation concentration is 0.01N.

the periphery so that the inter-microgel complexation is enhanced. In the cooling process, for Ca^{2+}, there is only a little hystersis, but for Cu^{2+}, $\langle R_h \rangle$ increases even when the temperature is lower than 32°C. It is interesting to note that for Cu^{2+}, the hystersis in $M_{w,aggregate}$ is not as large as that in $\langle R_h \rangle$, revealing a partial dissociation of the aggregates at lower temperatures. In the case of Hg^{2+}, there was a large hystersis in the cooling. $M_{w,aggregate}$ remained nearly constant in the cooling process, indicating a strong inter-microgel complexation between Hg^{2+} and COO^- groups. The fact that there was nearly no increase of $\langle R_h \rangle$ in the cooling revealed a strong intra-microgel complexation.

Fig. 7 shows that after reducing the cation concentration to 0.0025N, the results are quite different from those shown in Figs. 3 and 4, especially, for Hg^{2+}. In the range 25–32°C, the shrinking of microgels is similar to the case of adding 0.01N cations, expect for Hg^{2+}. The increases of $\langle R_h \rangle$ and $M_{w,aggregate}$ in the temperature range ~30–33°C indicated an inter-microgel aggregation. It is interesting to see that a further increase in temperature results in a decrease in $\langle R_h \rangle$ even though $M_{w,aggregate}$ still increases. This is because at higher temperatures, the effect of the intra-microgel hydrophobic attraction is stronger than the inter-microgel complexation. In the cooling process, the Ca^{2+} induced aggregation is essentially reversible, but there exists a large hysteresis in the Cu^{2+} or Hg^{2+} induced aggregation because of a strong complexation between Cu^{2+} and Hg^{2+} with COO^- groups. It is known that in terms of the strength of the complexation between the divalent cations and COO^- groups, $Hg^{2+} \gg Cu^{2+} > Ca^{2+}$. However, Fig. 7 shows that the extent of the inter-microgel complexation induced by Cu^{2+} is higher than that by Hg^{2+}. This clearly shows that in order to induce the inter-microgel complexation, there exists an optimal strength of the complexation between the cation and COO^- groups. If the strength of the complexation is too strong, the intra-microgel complexation will lead to much less inter-microgel complexation. On the other hand, if the strength of the complexation is too weak, the attraction between the cation and COO^- groups will not be sufficient to pull different microgels together. In our envisioned biomedical applications, this finding is very important for the cation-induced gelation of the microgels.

Fig. 8 shows the kinetics of the microgel aggregation induced by Ca^{2+} and Cu^{2+} at 32.5°C in terms of the relative average hydrodynamic volume $\langle V_h \rangle / \langle V_h \rangle_0$ and the relative weight average molar mass $M_{w,aggregate}/(M_{w,aggregate})_0$, where $\langle V_h \rangle$ is defined as $(4\pi/3)\langle R_h \rangle^3$. Both $\langle V_h \rangle / \langle V_h \rangle_0$ and $M_{w,aggregate}/(M_{w,aggregate})_0$ increase linearly with time before they reach the plateaus, indicating that the chain density remains a constant in the process. On the basis of Fig. 8, we found that the average chain densities for the Ca^{2+} or Cu^{2+} induced aggregates are 0.20 and 0.24 g/cm^3, respectively. This indicates that the aggregation is a diffusion-controlled process in which individual microgels are pulled to the aggregate in a one-by-one fashion. The changes of both $\langle V_h \rangle / \langle V_h \rangle_0$ and $M_{w,aggregate}/(M_{w,aggregate})_0$ reveal that the

inter-microgel complexation induced by Cu^{2+} is fast than that by Ca^{2+}. Such a trend in the strength of the cation induced complexation is similar to that derived from Pearson's concept of hard-and-soft acids and bases [23]. Generally, hard acids coordinate better with hard bases and soft acids with soft bases. The hard base–hard acid interaction is a charge-controlled one, resulting mostly from a favorable electrostatic interaction between a donor and an acceptor, respectively, with a high and a low orbital electronegativity. However, the interaction between a soft acid and a soft base normally leads to the covalent coordination of a donor with a low orbital electronegativity and an acceptor with a high orbital electronegativity [24]. In the present system, the COO^- groups is a soft base and the cations Hg^{2+} and Cu^{2+} are soft acids, but the cation Ca^{2+} is in the borderline between hard and soft acids. The Hg^{2+} or Cu^{2+} induced complexation is a typical soft base–soft acid interaction so that it is stronger.

4. Conclusions

Our results reveal that using a combination of cation and temperature, we can manipulate the balance between the hydrophobic interaction and the cation/COO^- complexation and the balance between the inter- and intra-microgel complexation, so that the aggregation of the P(VCL-*co*-SA) microgels can be induced in a controllable fashion. At temperatures lower than 32°C, divalent cations induce only the intra-microgel complexation with the COO^- groups, leading to the shrinking of the microgel, while at higher temperatures, the complexation of divalent cations with the COO^- groups forced on the periphery results in the inter-microgel aggregation. The strength of the complexation follows the order of $Hg^{2+} \gg Cu^{2+} > Ca^{2+}$. For a given cation concentration, the Ca^{2+} induced aggregation is essentially reversible in the heating-and-cooling cycle, but there exists a large hysteresis in the Cu^{2+} induced one because the complexation between Cu^{2+} and COO^- groups is stronger. As expected, the monovalent Na^+ was not able to induce the intra- or inter-microgel aggregation via the complexation. On the other hand, the intra-microgel complexation induced by Hg^{2+} is so strong that the inter-microgel aggregation is hindered because of the lack of COO^- groups on the periphery of the microgel at higher temperatures, if Hg^{2+} was added before increasing the temperature. Therefore, in order to enhance the inter-microgel aggregation, the strength of the complexation between the cation and COO^- groups have to be optimized.

Acknowledgements

Financial support of the Research Grants Council of the Hong Kong Special Administration Region Earmarked Grant 1999/2000 (CUHK 4209/99P, 2160122) and of NNSFC 29974027 is gratefully acknowledged.

References

[1] Porasso RD, Benegas JC, Van den Hoop MGT. J Phys Chem B 1999;103:2361–5.
[2] Ershov BG, Henglein A. J Phys Chem B 1998;102:10663–6.
[3] Ikeda Y, Beer M, Schmidt M, Huber K. Macromolecules 1998;31:728–33.
[4] Heitz C, Francois J. Polymer 1999;40(12):3331–44.
[5] Peng S, Wu C. Macromol Symp 2000;159(6):179–86.
[6] Wall FT, Drenan JW. J Polym Sci 1951;7:83–8.
[7] Flory PJ, Osterheld JE. J Phys Chem 1954;58:653–61.
[8] Fracex PI, Haas SM. J Nutr 1977;107:1889–95.
[9] Prohaska IR, Zukasewycz OA. Science 1983;213:559–61.
[10] Rotnenbacher H, Schermann H. J Nutr 1980;110:1648–52.
[11] Hart DA. Cell Immunol 1982;71(1):159–68.
[12] Frank HS, Wen WY. Discuss Faraday Trans 1978;74:583–7.
[13] James DW, Frost RL. J Chem Soc Faraday Trans 1976;80(12):1346–50.
[14] Hindman JC. J Chem Phys 1962;36:1000–15.
[15] Peng S, Wu C. Macromolecules 1999;32:585–9.
[16] Gao Y, Au-Yeung SZ, Wu C. Macromolecules 1999;32:3674–7.
[17] Sekikawa H, Hori R, Arita T, Ito K, Nakano M. Chem Pharm Bull 1978;26:2489–95.
[18] Ciardelli F, Tsuchida E, Wohrle D, editors. Macromolecule–metal complexes. Berlin: Springer, 1996.
[19] Wang X, Xu Z, Wan Y, Huang T, Pispas S, Mays JW, Wu C. Macromolecules 1997;30:7202–5.
[20] Berne BJ, Pecora R. Dynamic light scattering. New York: Plenum Press, 1976.
[21] Chu B. Laser light scattering. 2nd ed. New York: Academic Press, 1991.
[22] Stockmayer WH, Schmidit M. Pure Appl Chem 1982;54:407–14.
[23] Pearson RG. J Chem Educ 1968;45(9):581–7.
[24] Klopman G. Chemical reactivity and reaction path. New York: Wiley, 1974.